



Ultrafine Entanglement Witnessing

Farid Shahandeh,^{1,*} Martin Ringbauer,^{1,2,†} Juan C. Loredó,^{1,2} and Timothy C. Ralph¹

¹Centre for Quantum Computation and Communication Technology, School of Mathematics and Physics, University of Queensland, Brisbane, Queensland 4072, Australia

²Centre for Engineered Quantum Systems, School of Mathematics and Physics, University of Queensland, Brisbane, Queensland 4072, Australia

(Received 13 October 2016; published 14 March 2017)

Entanglement witnesses are invaluable for efficient quantum entanglement certification without the need for expensive quantum state tomography. Yet, standard entanglement witnessing requires multiple measurements and its bounds can be elusive as a result of experimental imperfections. Here, we introduce and demonstrate a novel procedure for entanglement detection which simply and seamlessly improves any standard witnessing procedure by using additional available information to tighten the witnessing bounds. Moreover, by relaxing the requirements on the witness operators, our method removes the general need for the difficult task of witness decomposition into local observables. We experimentally demonstrate entanglement detection with our approach using a separable test operator and a simple fixed measurement device for each agent. Finally, we show that the method can be generalized to higher-dimensional and multipartite cases with a complexity that scales linearly with the number of parties.

DOI: 10.1103/PhysRevLett.118.110502

Quantum entanglement provides many advantages beyond classical limits, including quantum communication, computation, and information processing [1,2]. Yet, determining whether a given quantum state is entangled or not is a theoretically and experimentally challenging task [3,4]. In particular, the ideal approach of reconstructing the full quantum state via quantum tomography is practically infeasible for all but the smallest systems.

An elegant solution to this problem, known as entanglement witnessing, relies on the geometry of the set of nonentangled (separable) quantum states [2,5–7]. Since these states form a convex set, it is always possible to find a hyperplane such that a given entangled state lies on one side of the hyperplane, while all separable states are on the other side, see Fig. 1. This hyperplane is a so-called *entanglement witness* (EW) and corresponds to a joint observable that has a bounded expectation value over all separable quantum states. Any quantum state that produces a value beyond the bound must be entangled. This simplification, however, comes at a cost: first, different entangled states in general require different EWs to be detected; second, not every EW can be practically realized, i.e., can be decomposed into operators corresponding to available local measurement devices (See also Refs. [7–9] for examples of the reverse procedure: constructing EWs from local observables); third, when such a decomposition is possible, it might require multiple measurement devices (with multiple settings) to be implemented; and fourth, witnessing bounds can be elusive in the presence of experimental imperfections. Consequently, the goal is to construct EWs that have a simple decomposition and, at the same time, detect a large set of entangled states.

There are three main techniques to improve EWs. First, adding nonlinear terms to the original witness operator [10]; second, using collective measurements of EWs on multiple copies of the quantum state [11]; and third, optimizing a given witness to tighten the bound on the statistics of separable states as much as possible [12,13]. The latter, which we refer to as standard entanglement witnessing (SEW), is the most common procedure and can be used as a complementary procedure to the first two techniques. In SEW, one first evaluates the supremum (infimum) expectation value of the witness observable for all separable states. The witness operator is then decomposed into local measurements, such that its expectation

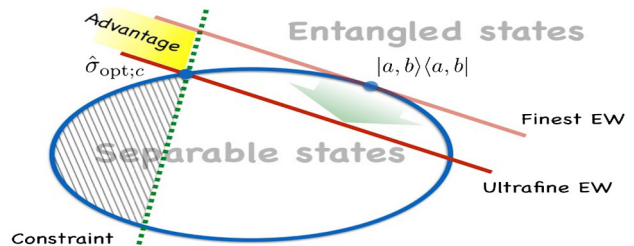


FIG. 1. In a standard witnessing, the *finest* entanglement witness (EW) is obtained by shifting a *test* operator so that its corresponding hyperplane becomes tangent to the set of separable states, and thus, optimal with respect to this set. However, additional information or constraints on the quantum states under investigation can effectively reduce the size of the candidate separable states (the hashed subset). Our technique takes this into account to provide an *ultrafine EW* that is tangent to this reduced set of separable states. This, in general, leads to an advantage over the standard procedure (the yellow region). By varying the constraint, one can scan a large range of entangled states.

value can be retrieved from the local measurement statistics. A comparison against the corresponding upper (lower) bound for separable states establishes the entanglement of the tested state. Crucially, a significant amount of information from these measurements remains unused by combining the statistics.

In this Letter, we introduce and demonstrate a novel approach for witnessing quantum entanglement that makes use of this otherwise unused additional information to seamlessly and inelaborately enhance any existing witnessing protocol. Our method, which we call *ultrafine entanglement witnessing* (UEW), relaxes the requirements on the test operators, which facilitates entanglement detection of a wide range of states, even if no witness decomposition in the common sense is provided. Moreover, our approach makes it possible to detect entanglement using only a simple measurement device for each party with the minimal number of measurements. We implement this technique experimentally on two-qubit entangled states shared by Alice and Bob, each of whom has access to a fixed three-outcome measurement device. Finally, we show that UEW can straightforwardly be extended to multipartite scenarios, with an experimental complexity that scales linearly with the number of parties involved.

Standard entanglement witnessing relies on the fact that the set of all separable states, \mathcal{S}_{sep} , is the collection of all convex combinations of pure product states. As a fruitful consequence of this convexity, we can identify quantum states outside \mathcal{S}_{sep} (i.e., entangled states) as follows. The Hahn-Banach theorem implies that for every entangled state $\hat{\rho}$ there exists a hyperplane that separates $\hat{\rho}$ from the set of separable states, see Fig. 1. Mathematically, there exists a Hermitian operator \hat{W} such that $\text{Tr}\hat{\rho}\hat{W} \geq 0$ for all $\hat{\rho} \in \mathcal{S}_{\text{sep}}$, while $\text{Tr}\hat{\rho}\hat{W} < 0$ [5]. In this sense, the operator \hat{W} , corresponding to the hyperplane discussed above, is an entanglement witness for $\hat{\rho}$.

Powerful EWs are most commonly constructed by optimizing a Hermitian (and possibly completely positive) test operator \hat{L} over the set of separable states as [12,13]

$$\hat{W} := g_s \hat{I} - \hat{L}, \quad (1)$$

where \hat{I} is the identity operator, and $g_s = \sup\{\text{Tr}\hat{L}\hat{\rho} : \hat{\rho} \in \mathcal{S}_{\text{sep}}\}$. Indeed, it is sufficient to optimize only over pure product states $|a, b\rangle$ [13]. One can also employ a similar recipe using the infimum value $g_i = \inf\{\text{Tr}\hat{L}\hat{\rho} : \hat{\rho} \in \mathcal{S}_{\text{sep}}\}$. This optimization procedure can be geometrically understood as translating the hyperplane corresponding to the test operator until it is tangent to the set of separable states, see Fig. 1. Hence, there exists an *optimal point* $|a, b\rangle$ for which $\langle a, b|\hat{W}|a, b\rangle = 0$ [7,14]. The resulting EW is said to be the *finest* witness in the sense that any further shift of its corresponding hyperplane will lead to an operator whose expectation value becomes negative for some

separable states, thus, violating the proper witnessing conditions [12,13].

It is, however, possible to significantly increase the detection power of any test operator by taking into account additional constraints and information about the states under investigation, which effectively reduces the size of the set of viable separable states, see Fig. 1. These constraints reflect physical restrictions on the measurement statistics that can be produced by separable states in certain situations. Similar considerations have previously been applied in the context of non-Gaussianity detection [15]. Consider, for example, a system composed of two spin-1/2 particles, which, in a measurement along the z axis, are always found either both with spin up or both with spin down. There is a large number of separable states that cannot produce such statistics and can thus be excluded from the optimization procedure for any witness aiming to detect the potential entanglement. Crucially, the required information about the state is already available, but not used, in almost every standard witnessing experiment.

Consider a Hermitian operator $\hat{C} \neq \hat{W}$ corresponding to some physical observable. Just like a witness, \hat{C} corresponds to a hyperplane splitting the space of all quantum states into two half-spaces $\mathcal{S}_c := \{\hat{\rho} : \text{Tr}\hat{C}\hat{\rho} \leq c\}$ and $\mathcal{S}_{\bar{c}} := \{\hat{\rho} : \text{Tr}\hat{C}\hat{\rho} \geq c\}$, where c is a real-valued free parameter. Depending on the choice of c , the hyperplane \hat{C} may or may not cut through the set of separable states, defining the two closed convex subsets $\mathcal{S}_{\text{sep};c} := \mathcal{S}_{\text{sep}} \cap \mathcal{S}_c = \{\hat{\rho} : \hat{\rho} \in \mathcal{S}_{\text{sep}} \text{ and } \text{Tr}\hat{C}\hat{\rho} \leq c\}$ and $\mathcal{S}_{\text{sep};\bar{c}} := \mathcal{S}_{\text{sep}} \cap \mathcal{S}_{\bar{c}} = \{\hat{\rho} : \hat{\rho} \in \mathcal{S}_{\text{sep}} \text{ and } \text{Tr}\hat{C}\hat{\rho} \geq c\}$. Clearly, whenever one of these sets is empty, the other one coincides with the set of all separable states, and hence, our method reduces to SEW. Therefore, in the following, we will consider parameter values for which both $\mathcal{S}_{\text{sep};c}$ and $\mathcal{S}_{\text{sep};\bar{c}}$ are nonempty. Using the test operator \hat{L} , one can now construct two EWs, \hat{W}_c and $\hat{W}_{\bar{c}}$, optimal to the sets $\mathcal{S}_{\text{sep};c}$ and $\mathcal{S}_{\text{sep};\bar{c}}$, respectively, by replacing g_s of Eq. (1) with $g_c = \sup\{\text{Tr}\hat{L}\hat{\rho} : \hat{\rho} \in \mathcal{S}_{\text{sep};c}\}$ and $g_{\bar{c}} = \sup\{\text{Tr}\hat{L}\hat{\rho} : \hat{\rho} \in \mathcal{S}_{\text{sep};\bar{c}}\}$. Consequently, a state $\hat{\rho}$ is entangled if

$$\text{Tr}\hat{C}\hat{\rho} \leq c \wedge \text{Tr}\hat{W}_c\hat{\rho} < 0, \text{ or, } \text{Tr}\hat{C}\hat{\rho} \geq c \wedge \text{Tr}\hat{W}_{\bar{c}}\hat{\rho} < 0. \quad (2)$$

Lemma 1.—Given a test operator \hat{L} with optimal points to the sets \mathcal{S}_{sep} and $\mathcal{S}_{\text{sep};X}$ as $|a, b\rangle$ and $\hat{\sigma}_{\text{opt};X}$ for $X = c, \bar{c}$, respectively, (i) If $\langle a, b|\hat{C}|a, b\rangle \leq c$, then $g_c = g_s$ and $\hat{\sigma}_{\text{opt};c} = |a, b\rangle\langle a, b|$, i.e., $\hat{W}_c = \hat{W}$. Furthermore, $\text{Tr}\hat{C}\hat{\sigma}_{\text{opt};\bar{c}} = c$. (ii) If $\langle a, b|\hat{C}|a, b\rangle \geq c$, then $g_{\bar{c}} = g_s$ and $\hat{\sigma}_{\text{opt};\bar{c}} = |a, b\rangle\langle a, b|$, i.e., $\hat{W}_{\bar{c}} = \hat{W}$. Furthermore, $\text{Tr}\hat{C}\hat{\sigma}_{\text{opt};c} = c$.

We point the interested reader to the Supplemental Material [16] for the proof of Lemma 1. Lemma 1 shows that the optimal point from SEW remains optimal for one of the two sets $\mathcal{S}_{\text{sep};X}$, while for the other set the optimal point

lies on the hyperplane \hat{C} , as visualized in Fig. 1. Hence, for a given c one of the conditions in Eq. (2) is advantageous over SEW. In addition, Eq. (2) together with Lemma 1 imply that UEW and SEW are equivalent only in the special case that the constraint value c is chosen exactly to match the expectation value of the constraint operator in the SEW optimal point, i.e., for $c = \langle a, b | \hat{C} | a, b \rangle$. Our strategy therefore never performs worse than SEW. Accordingly, we also obtain the following useful results, the proofs of which are provided in the Supplemental Material [16].

Theorem 1.—For a given constraint value c , the optimal state $\hat{\sigma}_{\text{opt};X} \in \mathcal{S}_{\text{sep};X}$ to the test operator \hat{L} is a pure state with $\text{Tr} \hat{C} \hat{\sigma}_{\text{opt};X} = c$.

Theorem 2.—The necessary condition for the separable operators \hat{C} and \hat{L} to detect entanglement via UEW is that $[\hat{C}, \hat{L}] \neq 0$.

Corollary 1.—If $\hat{C} = \hat{C}^A \otimes \hat{C}^B$ and $\hat{L} = \hat{L}^A \otimes \hat{L}^B$ are product operators, then \hat{C}^Y and \hat{L}^Y ($Y = A, B$) must not be jointly measurable [19,20].

In SEW, it is necessary that the test operator \hat{L} has an entangled eigenspace, since otherwise the supremum (and infimum) expectation values could be obtained by separable eigenstates. Theorem 2 and Corollary 1 show that our approach relaxes this requirement on the test operators and can be implemented with two separable (or even product) Hermitian operators. Notably, Corollary 1 implies that each party must use a measurement device with at least three outcomes, independent of the Hilbert space dimension of the system. In specific cases of bipartite and multipartite entanglement detection, this property can make UEW very efficient by significantly reducing the number of measurements.

Consider two parties, Alice and Bob, each of whom has access to a single measurement device $\mathcal{M}^A = \{\hat{\Pi}_i^A\}_{i=1}^n$, and $\mathcal{M}^B = \{\hat{\Pi}_i^B\}_{i=1}^m$, respectively, with $n, m \geq 3$. Indeed many strategies can be taken to implement SEW depending on \mathcal{M}^A and \mathcal{M}^B , while taking care that the obtained witness contains an entangled eigenspace [8,9]. To show that this is not a requirement of UEW, we give the following simple-to-construct example of a UEW strategy to detect a range of entangled states.

(i) Choose a constraint operator of the form $\hat{C} = \hat{\Pi}_i^A \otimes \hat{\Pi}_i^B$.

(ii) Choose a test operator of the form $\hat{L} = \hat{\Pi}_j^A \otimes \hat{\Pi}_j^B$ for $j \neq i$, such that \hat{L} and \hat{C} satisfy the conditions of Theorem 2 and Corollary 1.

(iii) For each value c , compute $g(c) = \sup\{\langle a, b | \hat{L} | a, b \rangle : |a, b\rangle \in \mathcal{S}_{\text{sep}}\}$ constrained to $\langle a, b | \hat{C} | a, b \rangle = c$.

(iv) The result is the concave *separability curve* $g(c)$. Any point above the curve indicates either of the conditions in Eq. (2), and thus, the entanglement of the corresponding state.

In the case where Alice and Bob use the same three-outcome measurement device with \hat{C} defined as above, there are six different separability curves. One of these

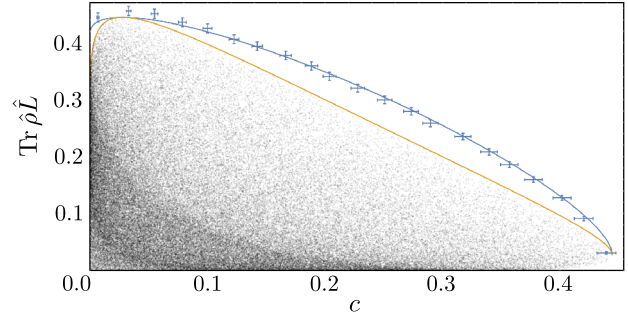


FIG. 2. Experimental results for ultrafine entanglement witnessing using the single measurement device defined in Eqs. (3) and (4) with $x = 2/3$ and $\theta = 0$. The separability curve, which represents the largest expectation values of the test operator obtainable from separable states, is shown in orange, while the maximal values obtainable with entangled states are represented by the blue curve. The blue data points correspond to 21 equispaced entangled states and include 3σ error bars. The black dots, obtained from randomly sampled pure product states with uniform distributions over the local Bloch spheres, illustrate the density of separable states with respect to the test and constraint operators. Note that the point where the orange and blue curves meet is the optimal point one would obtain for \hat{L} in SEW.

curves is shown in Fig. 2 together with the expectation and experimental observations for a family of entangled states. We emphasize here that, in general, arbitrary positive operator-valued measure (POVM) elements can be combined to form complex constraints and test operators. Moreover, one might consider using multiple constraints, which would lead to *separability hypersurfaces*. Hence, there is a large number of different possible ways to implement UEW.

Experimentally, we consider two-qubit states encoded in the polarization of single photons, shared between Alice and Bob. They are both equipped with a three-outcome measurement device as shown in Fig. 3, which implements the POVM elements

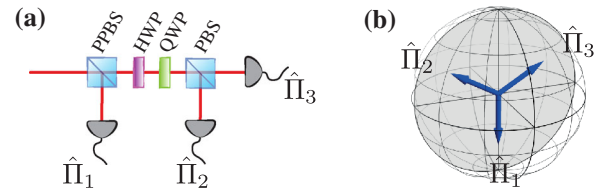


FIG. 3. (a) Experimental implementation of the three-outcome qubit measurement of Eq. (3). The first POVM element $\hat{\Pi}_1$ is implemented directly by a partially polarizing beam splitter (PPBS) with reflection coefficients $r_H = 0$ for horizontal and $r_V = 2/3$ for vertical polarization. The other POVM elements $\hat{\Pi}_2$ and $\hat{\Pi}_3$ are implemented using a set of quarter-wave plate (QWP), half-wave plate (HWP), and a polarizing beam splitter (PBS). (b) Visualization of our three-outcome POVM in the xz plane of the Bloch sphere.

$$\hat{\Pi}_1 = x|V\rangle\langle V|, \quad \hat{\Pi}_2 = |\chi^+\rangle\langle\chi^+|, \quad \hat{\Pi}_3 = |\chi^-\rangle\langle\chi^-|, \quad (3)$$

where $|\chi^\pm\rangle = (1/\sqrt{2})|H\rangle \pm e^{i\theta}\sqrt{1-x/2}|V\rangle$ with an arbitrary phase θ and $\sum_{i=1}^3 \hat{\Pi}_i = \hat{I}$. Alice and Bob then choose the test and constraint operators as

$$\hat{L} = \hat{\Pi}_2^A \otimes \hat{\Pi}_2^B, \quad \hat{C} = \hat{\Pi}_1^A \otimes \hat{\Pi}_1^B. \quad (4)$$

Since c must lie within the range of the expectation value of \hat{C} , Eqs. (3) and (4) imply that $0 \leq c \leq x^2$. The corresponding separability curve for the case $x = 2/3$ is shown in Fig. 2, together with a density plot of 10^5 separable states, randomly sampled from the uniform distribution of pure states on the local Bloch spheres. Equations (3) and (4) imply that in our experiment the constraint corresponds to a limit on the vertical polarization component.

Starting from a general pure state, we find that the maximal violation of the bound is obtained by states of the form

$$|\phi\rangle = \alpha|HH\rangle + \beta e^{-i\theta}|HV\rangle + \gamma e^{-i\theta}|VH\rangle + \delta|VV\rangle, \quad (5)$$

with $\alpha, \beta, \gamma, \delta \in \mathbb{R}$ satisfying $\alpha^2 + \beta^2 + \gamma^2 + \delta^2 = 1$. The requirement $\langle\phi|\hat{C}|\phi\rangle = c$ together with Eqs. (3) and (4) imply that $\delta = \sqrt{c}/x$. Maximizing the expectation value of the test operator is then equivalent to maximizing the overlap $\langle\chi^+\chi^+|\phi\rangle = \{\alpha + \sqrt{1-x}(\beta + \gamma) + \sqrt{c}[(1-x)/x]\}/2$. Since the last term is independent of the chosen state, we can assume $\beta = \gamma$, which reduces the problem to maximizing $\alpha/2 + \sqrt{1-x}\beta$ constrained to $\alpha^2 + 2\beta^2 = 1 - c/x^2$. For $x = 2/3$, one then obtains $\alpha_{\text{sup}} = \sqrt{3(4-9c)}/20$, $\beta_{\text{sup}} = \sqrt{(4-9c)}/20$, and the maximum expectation value of the test operator, $\sup\{\text{Tr}\hat{\rho}_{\text{ent}}\hat{L} : \text{Tr}\hat{\rho}_{\text{ent}}\hat{C} = c\} = (\alpha_{\text{sup}} + \sqrt{c}/2)^2$. Note that these values are independent of θ . Figure 2 shows the theoretical maximal violation curve, together with our experimental results for $\theta = 0$.

UEW can also be used to seamlessly and inelaborately improve any existing standard witnessing experiment: Consider two parties implementing a standard EW using the test operator $\hat{L} = \sum_{ij}\beta_{ij}\hat{\Pi}_i^A \otimes \hat{\Pi}_j^B$, where $\beta_{ij} \in \mathbb{R}$, and $\mathcal{M}^A = \{\hat{\Pi}_i^A\}_{i=1}^n$ and $\mathcal{M}^B = \{\hat{\Pi}_j^B\}_{j=1}^m$ ($n, m \geq 3$) are the local POVM elements of Alice and Bob, respectively. Their aim is to violate the inequality $\text{Tr}\hat{L}\hat{\rho} \leq g_s$ using an entangled state $\hat{\rho}$. After running the experiment many times and making lists of local measurement outcomes, Alice and Bob are able to compute the occurrence ratio of each joint element $\hat{\Pi}_i^A \otimes \hat{\Pi}_j^B$, and thus $\text{Tr}(\hat{\Pi}_i^A \otimes \hat{\Pi}_j^B)\hat{\rho}$. These values lead to the expectation value $\text{Tr}\hat{L}\hat{\rho}$. At this stage, they can also construct an arbitrary Hermitian constraint operator, say $\hat{C} = \sum_{ij}\gamma_{ij}\hat{\Pi}_i^A \otimes \hat{\Pi}_j^B$ ($\gamma_{ij} \in \mathbb{R}$), subject to the conditions of Theorem 2 and Corollary 1, and compute $\text{Tr}\hat{C}\hat{\rho}$ in exactly the same way using their already measured

expectation values. Upon obtaining $\text{Tr}\hat{C}\hat{\rho} = c$, they reoptimize \hat{L} over the set of pure product states with $\langle a, b|\hat{C}|a, b\rangle = c$ to obtain the new tighter bound $g(c) \leq g_s$ and test the inequality $\text{Tr}\hat{L}\hat{\rho} \leq g(c)$. Hence, every state $\hat{\rho}$ that violates the SEW inequality leads to an even stronger (and thus more robust) violation of the corresponding UEW bound. Notably, there are many (in fact, infinitely many) constraints that could be constructed from the measured POVM elements.

We now show how the simple procedure for UEW outlined above can be directly extended to the multipartite scenario, where a quantum state is shared between multiple parties. SEW, for this case, has been demonstrated in theory and experiment in Refs. [21,22]. Consider a N -qubit system shared between N agents, each of them having a three-outcome measurement device with POVM elements given by Eq. (3). Moreover, suppose that an arbitrary k partitioning of the system has been chosen as $\mathbf{P}_k = (\mathcal{I}_1|\mathcal{I}_2|\dots|\mathcal{I}_k)$, where each party \mathcal{I}_i is a subset of the index set $\mathcal{I} = \{1, 2, \dots, N\}$, containing $M_i = \text{card}\mathcal{I}_i$ agents (and hence, subsystems), so that $\sum_i \text{card}\mathcal{I}_i = \sum_i M_i = N$. Moreover, the list of parties is ordered such that $M_1 \leq M_2 \leq \dots \leq M_k$. Now, the agents chose the test and constraint operators as

$$\hat{L} = \bigotimes_{i=1}^k \hat{L}_i = \bigotimes_{i \in \mathcal{I}_1} \hat{\Pi}_2^{(i)} \otimes \bigotimes_{i \in \mathcal{I}_2} \hat{\Pi}_2^{(i)} \dots \otimes \bigotimes_{i \in \mathcal{I}_k} \hat{\Pi}_2^{(i)}, \quad (6)$$

$$\hat{C} = \bigotimes_{i=1}^k \hat{C}_i = \bigotimes_{i \in \mathcal{I}_1} \hat{\Pi}_1^{(i)} \otimes \bigotimes_{i \in \mathcal{I}_2} \hat{\Pi}_1^{(i)} \dots \otimes \bigotimes_{i \in \mathcal{I}_k} \hat{\Pi}_1^{(i)}, \quad (7)$$

implying $0 \leq c \leq x^N$.

As a proof of principle, suppose that $c = 0$. In the Supplemental Material [16], we prove that the maximum separable bound for a partition \mathbf{P}_k is given by

$$g(x; N, M_k) = \left(1 - \frac{x}{2}\right)^N - \left(1 - \frac{x}{2}\right)^{N-M_k} \left(\frac{1-x}{2}\right)^{M_k}. \quad (8)$$

Since the test and constraint operators are invariant under the exchange of agents between different parties, so is the bound $g(x; N, M_k)$. Three cases are of particular interest. First, if $M_k = N$, then no partitioning has been made and $g(x; N, N)$ represents the maximum expectation value of the test operator \hat{L} over all N -partite quantum states. Hence, this bound can not be violated by any quantum state. Second, if $M_k = N - 1$, the resulting bound corresponds to the bipartitions with one subsystem in one party and $N - 1$ subsystems in the other. One can easily see that for any bipartition with $M_k < N - 1$, $g(x; N, M_k) < g(x; N, N - 1)$. Consequently, any state violating this bound is entangled within all bipartitions and thus, genuinely N partite entangled. Finally, if $M_k = 1$, each party constitutes one agent corresponding to the partition with

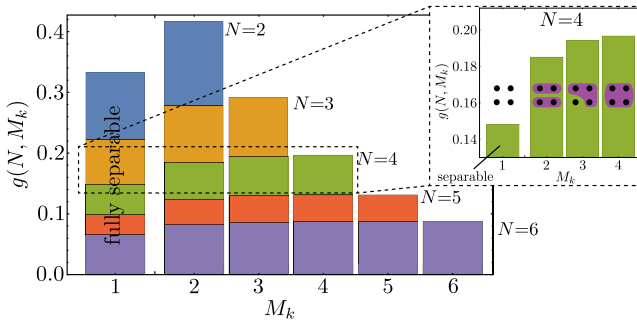


FIG. 4. The bounds $g(N, M_k)$ versus the cardinality of the largest party M_k for $2 \leq N \leq 6$, where each N is shown in a different color. For a state of interest with $c = 0$, a violation of the bound $g(N, 1)$ proves its (partial) entanglement, while a violation $g(N, N - 1)$ proves its genuine N -partite entanglement. The inset shows the case $N = 4$ with the four black dots representing the four subsystem and the purple shaded boxes visualize the maximally allowed entangled subset.

the highest resolution, i.e., \mathbf{P}_N . Thus, any state violating the bound $g(x; N, 1)$ is partially entangled.

Figure 4 shows $g(N, M_k) := g(\frac{2}{3}; N, M_k)$ versus the cardinality of the largest party M_k for $2 \leq N \leq 6$. As N increases, it becomes increasingly hard to detect genuine N -partite entanglement with the simplest version of our approach. However, detecting partial entanglement by violating the bound $g(N, 1)$ remains experimentally feasible for larger N . This example shows that our approach can be extended to the multipartite case, where it allows for simple entanglement detection with a number of measurements that scales as $3N$ with the number of agents N . For tomographic methods or Bell tests in contrast, the number of measurements scales exponentially with the number of qubits [23]. In fact, current EWs require at least $D + 1$ measurements for each agent, where D is the minimum Hilbert space dimension of the subsystems [21,24], while our technique provides the possibility of detecting entangled states using only three-outcome measurements independent of the Hilbert space dimensionality.

In conclusion, we have introduced a novel procedure for witnessing quantum entanglement using additional information that is typically already available in a standard witnessing experiment. Our ultrafine entanglement witnessing relaxes the requirements on the test operators and allows for entanglement detection with a much smaller number of measurements compared to the standard entanglement witnessing. This is a considerable experimental simplification which potentially allows for faster and more precise detection of entanglement compared to the existing protocols. We have demonstrated this in practice for a family of two-qubit entangled states using two fixed three-outcome POVMs. We also showed that our method always performs at least as well as the standard procedure and seamlessly and inelaborately improves it. We have described a scalable experimental protocol that generalizes

to higher dimensional and multipartite quantum systems, and showed that, in its simplest form, the number of measurements required for this protocol scales linearly with the number of agents.

The authors gratefully acknowledge A.G. White for helpful discussions and T. Vulpecula for experimental assistance. This project was supported by the ARC Centres for Quantum Computation and Communication Technology (CE110001027) and Engineered Quantum Systems (CE110001013).

*f.shahandeh@uq.edu.au

†m.ringbauer@uq.edu.au

- [1] M. A. Nielsen and I. L. Chuang, *Quantum Computation and Quantum Information* (Cambridge University Press, Cambridge, 2000).
- [2] R. Horodecki, P. Horodecki, M. Horodecki, and K. Horodecki, *Rev. Mod. Phys.* **81**, 865 (2009).
- [3] L. Gurvits, in *Proceedings of the Thirty-fifth Annual ACM Symposium on Theory of Computing, 2003* (ACM, New York, 2003), p. 10.
- [4] S. Gharibian, *Quantum Inf. Comput.* **10**, 343 (2010).
- [5] M. Horodecki, P. Horodecki, and R. Horodecki, *Phys. Lett. A* **223**, 1 (1996).
- [6] M. Horodecki, P. Horodecki, and R. Horodecki, *Phys. Lett. A* **283**, 1 (2001).
- [7] D. Chruściński and G. Sarbicki, *J. Phys. A* **47**, 483001 (2014).
- [8] S. Yu and N. L. Liu, *Phys. Rev. Lett.* **95**, 150504 (2005).
- [9] H. Gholipour and F. Shahandeh, *Phys. Rev. A* **93**, 062318 (2016).
- [10] O. Gühne and N. Lütkenhaus, *Phys. Rev. Lett.* **96**, 170502 (2006).
- [11] P. Horodecki, *Phys. Rev. A* **68**, 052101 (2003).
- [12] M. Lewenstein, B. Kraus, J. I. Cirac, and P. Horodecki, *Phys. Rev. A* **62**, 052310 (2000).
- [13] J. Sperling and W. Vogel, *Phys. Rev. A* **79**, 022318 (2009).
- [14] F. Shultz, *J. Math. Phys. (N.Y.)* **57**, 015218 (2016).
- [15] R. Filip and L. Mišta, *Phys. Rev. Lett.* **106**, 200401 (2011).
- [16] See Supplemental Material at <http://link.aps.org/supplemental/10.1103/PhysRevLett.118.110502>, which includes Refs. [17–19], for detailed proofs of Lemma 1, Theorem 1, Theorem 2, Corollary 1, and derivation of Eq. (8).
- [17] J. Sperling and W. Vogel, *Phys. Rev. A* **79**, 052313 (2009).
- [18] G. Cassinelli, E. De Vito, and A. Levrero, *J. Math. Anal. Appl.* **210**, 472 (1997).
- [19] P. Kruszynski and W. M. de Muynck, *J. Math. Phys. (N.Y.)* **28**, 1761 (1987).
- [20] Note that, two observables \hat{A} and \hat{B} are called jointly measurable if and only if a dilation of them into a larger Hilbert space results two operators \hat{A}_0 and \hat{B}_0 such that $[\hat{A}_0, \hat{B}_0] = 0$; see Ref. [19].
- [21] J. Sperling and W. Vogel, *Phys. Rev. Lett.* **111**, 110503 (2013).
- [22] S. Gerke, J. Sperling, W. Vogel, Y. Caciai, J. Roslund, N. Treps, and C. Fabre, *Phys. Rev. Lett.* **114**, 050501 (2015).
- [23] G. Tóth and O. Gühne, *Phys. Rev. Lett.* **94**, 060501 (2005).
- [24] O. Gühne, P. Hyllus, D. Bruss, A. Ekert, M. Lewenstein, C. Macchiavello, and A. Sanpera, *J. Mod. Opt.* **50**, 1079 (2003).